TABLE 1

Transmission coefficients, T_l, calculated with code ABACUS for α-particles on ^{29}Si at representative energies, E_α

T_l	E_α (MeV)							
	3.675	3.875	4.135	4.325	4.635	4.975	5.235	5.410
T_0	0.0686	0.1118	0.1869	0.2517	0.3639	0.4796	0.5556	0.5998
T_1	0.0291	0.0512	0.0967	0.1439	0.2459	0.3832	0.4932	0.5643
T_2	0.0257	0.0455	0.0854	0.1258	0.2096	0.3167	0.3995	0.4524
T_3	0.00510	0.00973	0.0206	0.0338	0.0688	0.1328	0.2024	0.2588
T_4	0.00232	0.00461	0.0101	0.0171	0.0359	0.0712	0.1103	0.1425
T_5	0.000227	0.000474	0.00113	0.00203	0.00485	0.0113	0.0204	0.0294
T_6	0.000054	0.000120	0.000306	0.000571	0.00143	0.00352	0.00651	0.00952
T_7	0.000003	0.000007	0.000019	0.000036	0.000099	0.000269	0.000542	0.000935

Care was taken in establishing this potential to see that the transmission coefficients were smooth functions of energy and angular momentum. Representative transmission coefficients calculated by code ABACUS are presented in table 1.

5. The ^{29}Si(α, n_0)^{32}S excitation functions and normalization procedure

The 0° and 160° excitation functions for the ^{29}Si(α, n_0)^{32}S reaction corrected for neutron background and detection efficiency are shown in fig. 4. On 42 of these resonances, angular distributions were then measured. Initially we concern ourselves only with those angular distributions that are associated with the excitation of a single state in the compound nucleus. Their spin values are readily identified from the unique shapes displayed by these distributions [11]). Unfortunately only seven resonances fall in this single-level category. Therefore, five mixed-level resonances where one of the two states is readily identified as the major cross-section contributor were also selected. These $\theta = 160°$ on-resonance cross sections converted to the c.m. system are plotted versus α-energy in fig. 5 as open symbols.

Differential cross sections calculated and normalized by code MIA are also displayed in fig. 5 as a function of energy and J^π. The single normalization factor of 1.333 multiplying the calculated cross sections brings the curves into approximate agreement with the measured values. Note the order of magnitude cross-section sensitivity to parity for $J \geqq \frac{5}{2}$.

Preliminary to this calculation the transmission coefficients for the competing neutron and proton channels were calculated by means of the computer code SCAT [ref. [12])] using the Wilmore-Hodgson potential [13]) modified to include a spin-orbit potential of 7.5 MeV and the Perey potential [14]) respectively. The α-particle transmission coefficients were discussed earlier.

These transmission coefficients were calculated for the significant channels given in fig. 6 and formed the input to program MANDYF [15]) in which the penetrability factors were calculated. Typical values of these ^{29}Si(α, n_0)^{32}S penetrability factors

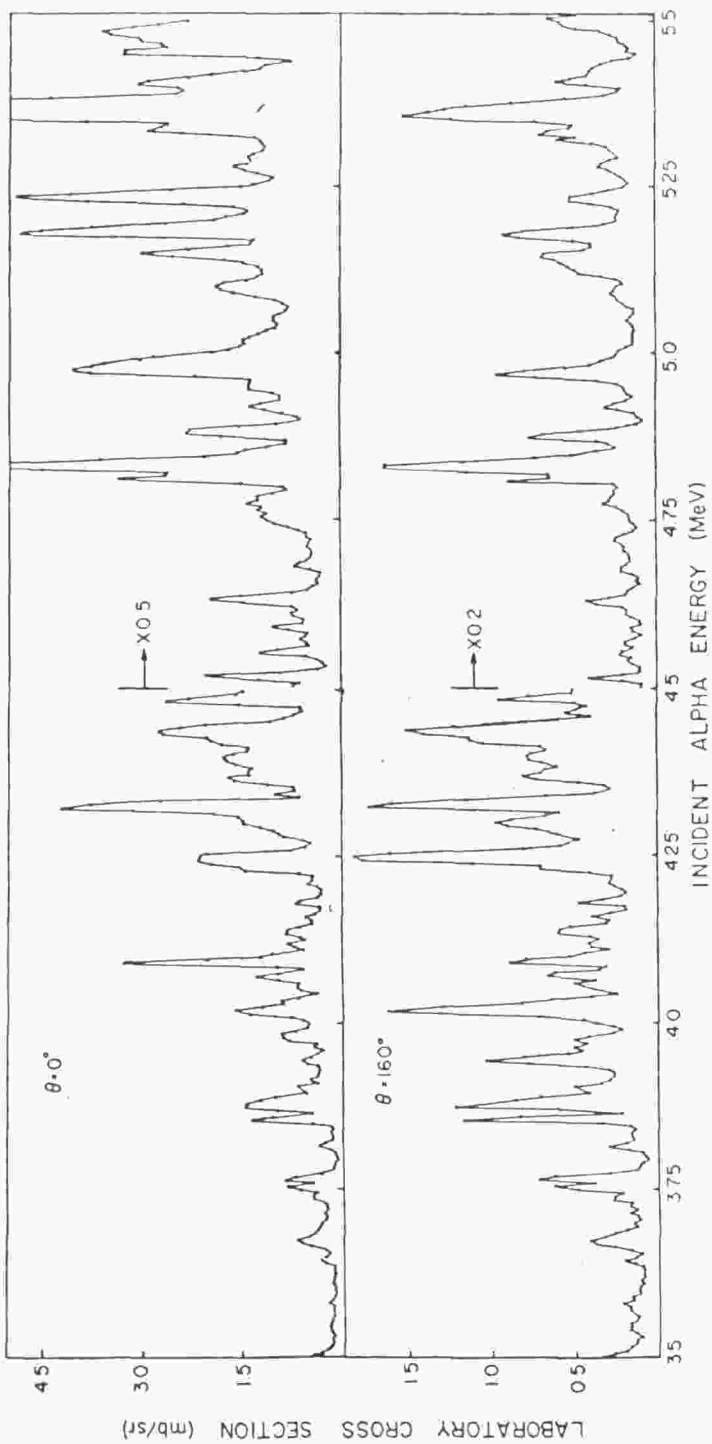

Fig. 4. Measured $^{29}Si(\alpha, n_0)^{32}S$ excitation functions at 0° and 160° laboratory angles over an α-energy range, E_α = 3.5–5.5 MeV.

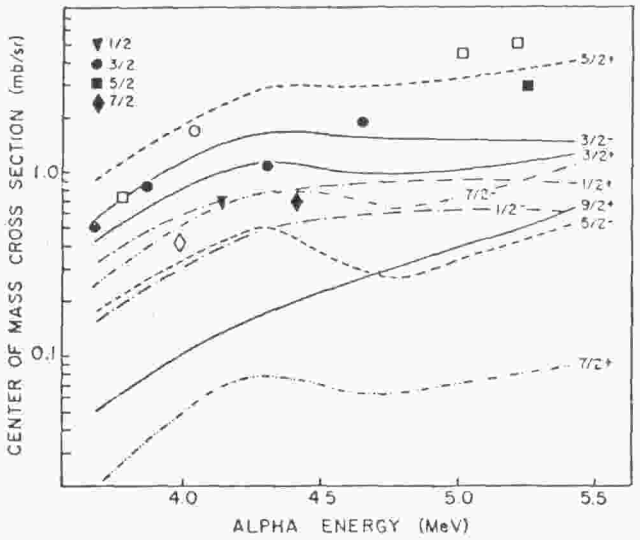

Fig. 5. Normalized theoretical $^{29}Si(\alpha, n_0)^{32}S$ excitation functions and measured on-resonance cross sections at 160° for spin $\frac{1}{2}$, $\frac{3}{2}$, $\frac{5}{2}$ and $\frac{7}{2}$ states in ^{33}S. Solid symbols indicate a pure, single-level resonance is measured whereas open symbols indicate that a secondary state is also contributing.

TABLE 2

Penetrability factors calculated with code MANDYF for the $^{29}Si(\alpha, n_0)^{32}S$ reaction at representative energies, E_x, for specific ^{33}S states, J^π

J^π	E_x (MeV)							
	3.675	3.875	4.135	4.325	4.635	4.920	5.235	5.410
$\frac{1}{2}^-$	0.0281	0.0479	0.0843	0.1158	0.1397	0.1580	0.1693	0.1715
$\frac{1}{2}^+$	0.0612	0.0929	0.1405	0.1739	0.2165	0.2373	0.2410	0.2374
$\frac{3}{2}^-$	0.0278	0.0470	0.0810	0.1086	0.0990	0.1035	0.1087	0.1102
$\frac{3}{2}^+$	0.0212	0.0335	0.0552	0.0714	0.0589	0.0701	0.0796	0.0830
$\frac{5}{2}^-$	0.0042	0.00711	0.0116	0.0153	0.00822	0.0114	0.0171	0.0214
$\frac{5}{2}^+$	0.0231	0.0384	0.0673	0.0924	0.0922	0.1170	0.1378	0.1471
$\frac{7}{2}^-$	0.00416	0.00716	0.0124	0.0170	0.0115	0.0156	0.0227	0.0279
$\frac{7}{2}^+$	0.000313	0.000282	0.000786	0.00106	0.00139	0.00165	0.00204	0.00235
$\frac{9}{2}^-$	0.000006	0.000009	0.000017	0.000041	0.000038	0.000045	0.000072	0.000088
$\frac{9}{2}^+$	0.000752	0.000938	0.000278	0.00324	0.00505	0.000720	0.00949	0.0115
$\frac{11}{2}^{-*}$	0.000010	0.000016	0.000031	0.000060	0.000081	0.000108	0.000195	0.000247
$\frac{11}{2}^+$	0.000000	0.000000	0.000000	0.000000	0.000000	0.000002	0.000002	0.000003

are listed in table 2. On the basis of their dependencies, the cross-section curves reflect a sensitivity to energy and J^π value of the ^{33}S compound nucleus state.

6. Analysis of on-resonance angular distributions

Early in these studies, we established the importance of measuring as full, detailed, and precise an angular distribution as possible on each resonance if a meaningful